2. THE MILKY WAY GALAXY

Matthew Baring – Lecture Notes for ASTR 360, Spring 2025

1 Historical Models of the Milky Way

• Early models of the visible stellar population were based on star counts, and pre-dated the concept of galaxies. They dealt with the distribution of relatively nearby stars, i.e. did not extend beyond the Milky Way. **C & O, Sec. 24.1**

• The non-uniformity of the band of Milky Way stars was first appreciated by Galileo, and it was Kant and Wright in the mid-1700s who first arrived at the concept of a disk population of stars.

• William Herschel first used star counts to explore the 3D distribution of stars in the 1780s. His research invoked 4 critical assumptions:

∗ (1) all stars emit at approximately the same absolute magnitude (= **standard candle** or narrow luminosity function assumption) [`fairly good`];

∗ (2) the number density of stars in space is roughly constant [`a uniformity that is realized on scales larger than a few parsecs`];

∗ (3) there is nothing between the stars to obscure them [`particularly flawed and critical at red wavelengths`];

∗ (4) he could see to the edge of the stellar distribution [`not true, but not damaging`].

• Herschel's inferences were of a disk-like distribution of stars that were roughly centered on the Sun.

- Kapteyn confirmed Herschel's results in 1920, but was able to quantify it better by *providing a distance scale* to the population.

Plot: The Kapteyn Universe

∗ Kapteyn's inference was for a *flattened spheroidal system* of stars that was virtually **heliocentric**. He used the **distance modulus** under a standard candle assumption to map out stellar distances.

∗ The semi-major axis of this spheroid was around 8.5kpc, and its minor axis was only 150 pc.

- During 1915-1919, Shapley estimated distances to 93 globular clusters (GCs) using RR Lyrae and W Virginis variable stars and their period-luminosity relation (*mention sound wave physics,* $t_s \sim 1/\sqrt{G\rho}$).

Plot: Cepheid Variable Period-Luminosity Relation

∗ He found that GCs are not distributed uniformly, but are centered around the constellation Sagittarius, and at distances at least around 15 kpc from the sun. The most distant GCs were around 100 kpc away.

- Both Kapteyn's and Shapley's scenarios were in error, Kapteyn's being too small and heliocentric; Shapley's being too large. Both were strongly influenced by the neglect of **interstellar extinction**.

∗ Extinction acts to obscure more distant regions, particularly in the disk (Kapteyn's preferential sample), and so leads to overestimates of population distance scales – stars are fainter because of extinction.

- In contrast, Shapley's results, which sampled high latitude GCs that experience much less extinction, suffered from a mis-calibration of the period-luminosity relation that used disk stars without properly correcting for extinction. On average, this overestimated the distances to clusters.

∗ Note that Shapley identified a **zone of avoidance** of GCs within 10° of the Galactic Plane. Shapley attributed this apparent anisotropy to strong gravitational tidal effects, whereas in reality it was caused by extinction.

The Kapteyn "Universe"

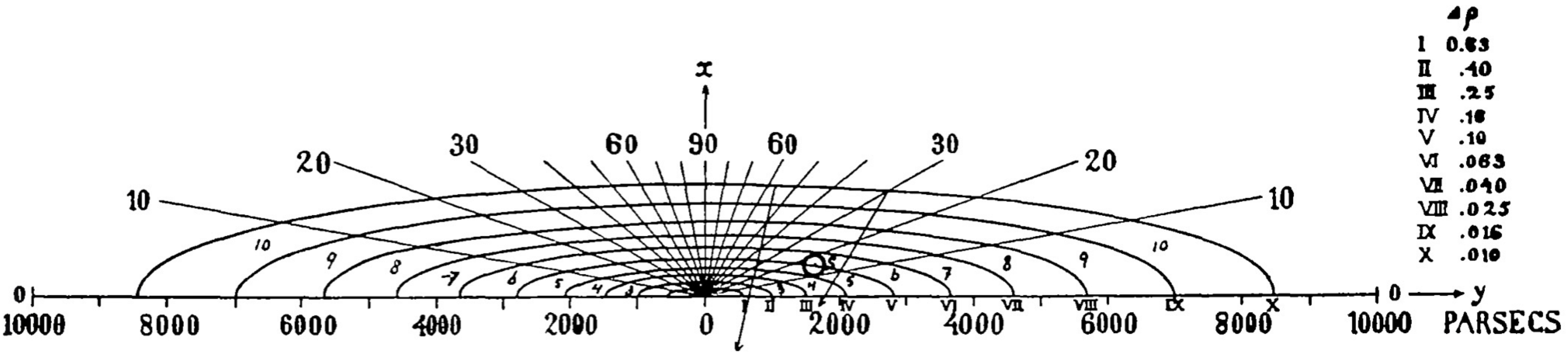

- Kapteyn's observational (distance modulus) stellar data on the universe as it was known in 1922, essentially just the Milky Way galaxy. The contours are of stellar density.
- Fig. 1 from Kapteyn (1922, ApJ, **55**, 302).

Cepheid Period-Luminosity Relation

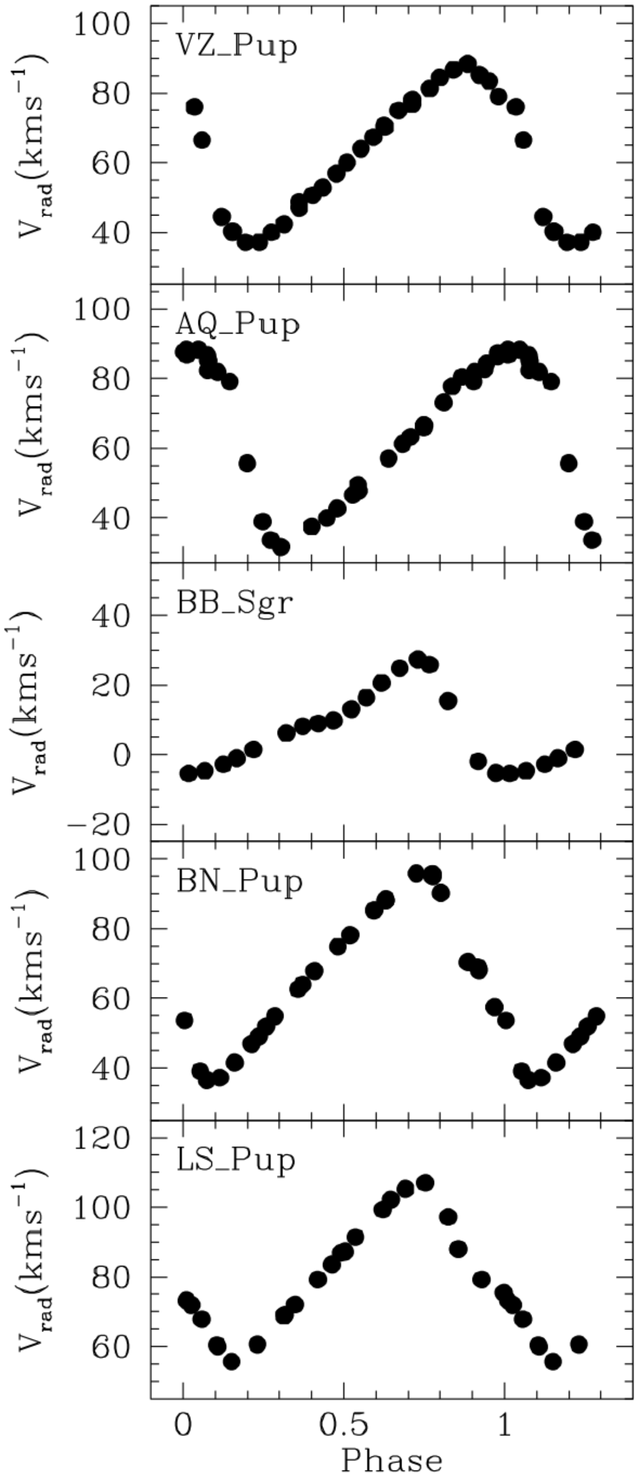

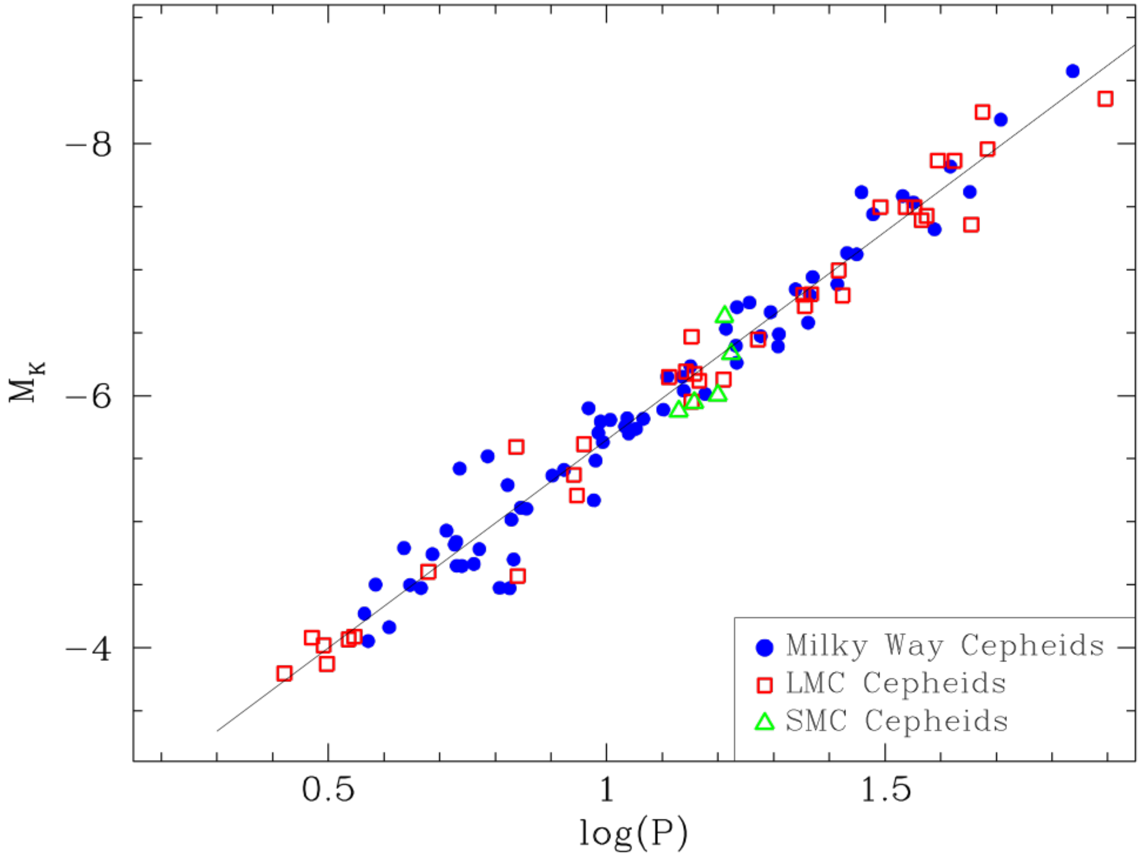

- *Left*: radial velocity curves for Milky Way Cepheids.
- *Top*: The Period-Luminosity relation in the K-band for the complete sample of Milky Way, LMC and SMC Cepheids having IRSB-determined distances.
- Storm et al. A&A (2011).

1.1 Star Counts and the $\log N - \log S$ Distribution

- The formalism for differential distributions of star counts in terms of observed magnitudes is largely dry, unelucidating, and is laid out in the text. It is suitable for a leisurely reading.

[*Reading Assignment: Differential and Integrated Star Counts, pp. 878–881*]

- Of greater insight is the $\mathbf{\log N - \log S}$ **distribution**, the standard tool for determining inhomogeneity in spatial populations. For a **standard candle** assumption, for which the **luminosity function** $f(L)$ of stars is narrow, we can approximate it via

$$f(L) \; = \; \delta(L - L_0) \quad . \tag{1}$$

This is a good approximation for a particular subset of main sequence stars. Then the observed flux S for sources at distance d from Earth is

$$S \; \equiv \; \mathcal{F} \; = \; \frac{L_0}{4\pi d^2} \quad \Rightarrow \quad d \; \propto \; \frac{1}{\sqrt{S}} \quad . \tag{2}$$

The *cumulative* number of sources $N(> S)$ observed to exceed a flux S is given by the total volume sampled out to distance d, *if isotropy and homogeneity* is assumed:

$$N(> S) \; \propto \; \int_{r \leq d} r^2 \, dr \; \propto \; d^3 \; \propto \; S^{-3/2} \quad . \tag{3}$$

Hence, for Euclidean geometry and isotropy, we have the classical result for the $\log N - \log S$ distribution:

$$\boxed{N(> S) \; \propto \; S^{-3/2} \quad .} \tag{4}$$

Non-Euclidean cosmological geometry modifies this result: e.g. the discussion of **gamma-ray bursts**.

Plot: $\log N - \log S$ Distributions for Inhomogeneous Populations

- The number drops off at lower values of S when the edge of the distribution is sampled: the peel-off point marks the volume of the distribution.

Log N – Log S in Euclidean Space

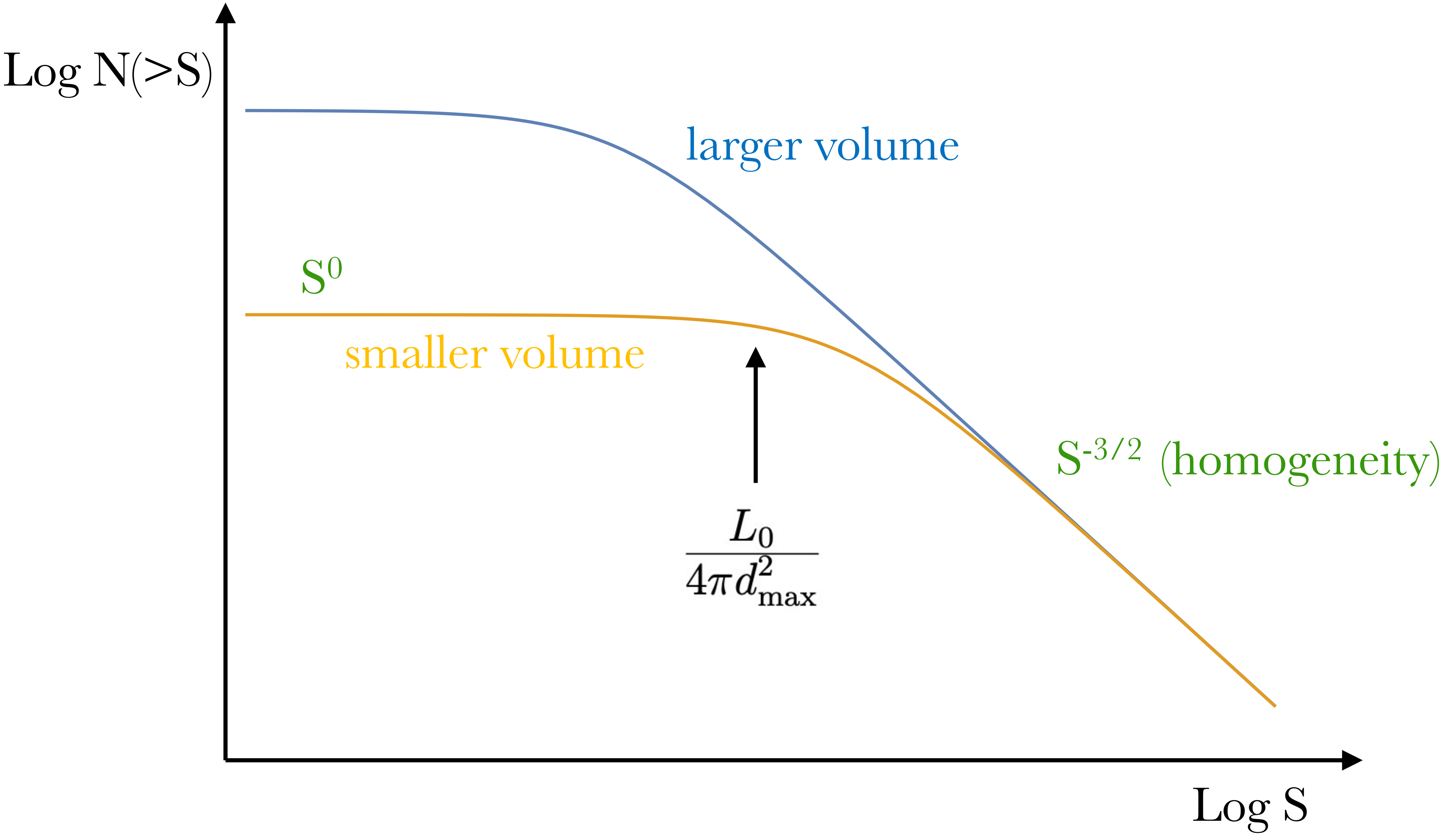

2 The Morphology of the Galaxy

- The perception of the Milky Way geometry has been refined over the last century to reveal a number of various components, as outlined below.

C & O, Sec. 24.2

$\boxed{\textbf{Plot:}}$ Diagram of the Galaxy

- The **solar galactocentric distance** has been continually revised downwards from Shapley's first estimate, and the current IAU designated value (1985) is 8.5 kpc. More recent work suggests a slightly lower value of 8 kpc.

- The matter distribution comprises disk-like and spheroidal components.

$\boxed{\textbf{Plot:}}$ Table of Disk and Spheroid Component Parameters

- The **disk** portion of the Milky Way is actually composed of several major components: a **young, thin disk** of vertical (exponential) scaleheight of 50pc, on **old thin disk** of scaleheight $z_{thin} \sim 325\,\text{pc}$, and thick disk of scaleheight $z_{thick} \sim 1.4\,\text{kpc}$.

$*$ The thick disk constitutes only 2 percent of disk stars, so that the density profile of stars in the disk, in cylindrical coordinates, can be written

$$n(z, R) \;\propto\; \Bigl\{ e^{-z/h_{thin}} + 0.02 e^{-z/h_{thick}} \Bigr\}\, e^{-R/h_R} \quad . \tag{5}$$

Here $h_R \sim 3.5\,\text{kpc}$ is the radial fall-off scale of the disk stellar density.

$*$ Exponential density declines are expected in uniform gravity zones with spatially-independent $\mathbf{g}$ (c.f. Earth's atmosphere) – they are supported by *stellar gravitational collision pressure*, an analog to gas molecule pressure.

$*$ Convention dictates that cylindrical coordinates (R, z) are employed in describing spatial locations in the Milky Way.

- The vertical **luminosity profile** possesses somewhat different scaleheights, suggesting that there is *a latitudinal dependence of mean stellar mass.*

- The components are distinguished also by chemical composition and kinematics properties. **Velocity dispersions** $\sigma = \sqrt{\langle v^2 \rangle}$ are generally greater at greater scale heights, a must for a self-gravitating system.

Schematic of the Milky Way

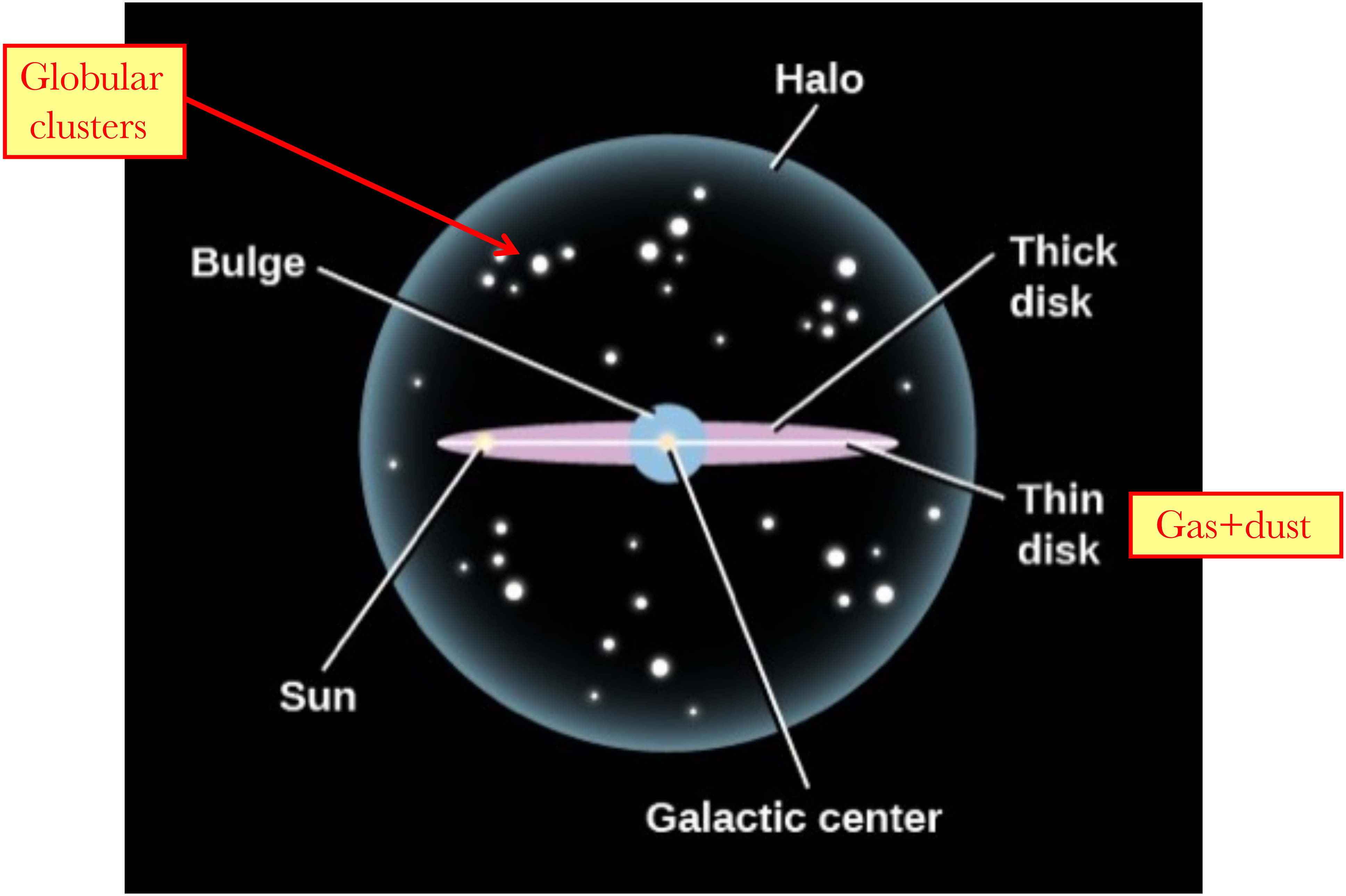

TABLE 24.1 Approximate Values for Various Parameters Associated with the Components of the Milky Way Galaxy. Definitions and details are discussed in the text.

	Disks		
	Neutral Gas	Thin Disk	Thick Disk
M (10^{10} $\mathrm{M}_\odot$)	0.5[a]	6	0.2 to 0.4
L_B (10^{10} $\mathrm{L}_\odot$)[b]	—	1.8	0.02
M/L_B ($\mathrm{M}_\odot/\mathrm{L}_\odot$)	—	3	—
Radius (kpc)	25	25	25
Form	e^{-z/h_z}	e^{-z/h_z}	e^{-z/h_z}
Scale height (kpc)	< 0.1	0.35	1
σ_w (km s^{-1})	5	16	35
[Fe/H]	$> +0.1$	-0.5 to $+0.3$	-2.2 to -0.5
Age (Gyr)	$\lesssim 10$	8[c]	10[d]

	Spheroids		
	Central Bulge[e]	Stellar Halo	Dark-Matter Halo
M (10^{10} $\mathrm{M}_\odot$)	1	0.3	190^{+360}_{-170}[f]
L_B (10^{10} $\mathrm{L}_\odot$)[b]	0.3	0.1	0
M/L_B ($\mathrm{M}_\odot/\mathrm{L}_\odot$)	3	~ 1	—
Radius (kpc)	4	> 100	> 230
Form	boxy with bar	$r^{-3.5}$	$(r/a)^{-1}\,(1 + r/a)^{-2}$
Scale height (kpc)	0.1 to 0.5[g]	3	170
σ_w (km s^{-1})	55 to 130[h]	95	—
[Fe/H]	-2 to 0.5	< -5.4 to -0.5	—
Age (Gyr)	< 0.2 to 10	11 to 13	~ 13.5

[a] $M_{\mathrm{dust}}/M_{\mathrm{gas}} \simeq 0.007$.

[b] The total luminosity of the Galaxy is $L_{B,\mathrm{tot}} = 2.3 \pm 0.6 \times 10^{10}\ \mathrm{L}_\odot$, $L_{\mathrm{bol,tot}} = 3.6 \times 10^{10}\ \mathrm{L}_\odot$ ($\sim 30\%$ in IR).

[c] Some open clusters associated with the thin disk may exceed 10 Gyr.

[d] Major star formation in the thick disk may have occurred 7–8 Gyr ago.

[e] The mass of the black hole in Sgr A* is $M_{\mathrm{bh}} = 3.7 \pm 0.2 \times 10^6\ \mathrm{M}_\odot$.

[f] $M = 5.4^{+0.2}_{-3.6} \times 10^{11}\ \mathrm{M}_\odot$ within 50 kpc of the center.

[g] Bulge scale heights depend on age of stars: 100 pc for young stars, 500 pc for old stars.

[h] Dispersions increase from 55 km s^{-1} at 5 pc to 130 km s^{-1} at 200 pc.

• The disk components also exhibit different **metallicities**. The metallicity is often defined to be the ion-to-hydrogen ratio, as inferred from spectroscopic measurements in stellar atmospheres:

C & O, pp. 885-6

$$[Fe/H] \;=\; \log_{10} \frac{(N_{Fe}/N_H)_{\rm star}}{(N_{Fe}/N_H)_\odot} \quad . \tag{6}$$

Iron is a good indicator, though often oxygen metallicities are employed as an equally useful indicator.

• Stellar evolution generally promotes an increase in Fe abundance after a number of cycles of supernovae from massive stars, so one naturally expects a correlation of age with metallicity - the **age-metallicity relation**.

∗ metal-rich (Population I) stars tend to be younger than metal-poor (Population II) ones, reflecting the faster evolution of more massive stars.

∗ But, SN explosions prepare the stellar formation environment, and chemical mixing of these regions is often incomplete. Hence, age inferences from $[Fe/H]$ and $[O/H]$ ratios can often be misleading or overly simplistic.

• Thick disk stars posses lower metallicity on average ($-0.6 < [Fe/H] < -0.4$), and are, by inference, older – this is consistent with higher velocity dispersion constraints on ages. Thin disk stars with $-0.4 < [Fe/H] < 0.3$ are assumed to be younger.

∗ Star count evidence for the thick disk only emerged during the 1980s, and uncertainties are still considerable.

• The **mass-to-light ratio** of thin disk stars is generally larger than for the sun. Since, for main sequence stars,

$$\frac{L}{L_\odot} \;=\; \left(\frac{M}{M_\odot} \right)^\alpha \quad , \tag{7}$$

with $\alpha \sim 4$ for $M \gtrsim 0.5 M_\odot$, and $\alpha \sim 2.3$ for $M \lesssim 0.5 M_\odot$, higher mass-to-light ratios generally correspond to more massive stars.

∗ This leads to the inference that the mean mass of stars in the thin disk is around $0.7 M_\odot$, which is a significant constraint on the initial mass function:

∗ ⇒ most stars in the disk are formed with sub-solar masses.

- Neutral hydrogen (21cm) maps, OB stellar associations, and open clusters can be used as tracers of Galactic structure. They reveal **spiral structure** that is not unlike that of the spiral galaxy M100 from the Messier catalogue.

C & O, pp. 887-90

$\boxed{\textbf{Plot:}}$ Spiral Galaxy M100 from the Hubble Space Telescope

∗ Spiral structure is more discernible in blue light (OB stars), but is not as evident in the red, which is characteristic of older, low mass stars.

∗ The sun is located in the Orion-Cygnus arm (or spur)

Spiral Galaxy M100 (NGC 4321) in Virgo from the Hubble Space Telescope